Rapid submarine melting driven by subglacial discharge, LeConte Glacier, Alaska

Roman J Motyka,[1,2] William P Dryer,[1,2] Jason Amundson,[2] Martin Truffer,[1] and Mark Fahnestock[1]

Received 30 July 2013; revised 26 September 2013; accepted 27 September 2013.

[1] We show that subglacial freshwater discharge is the principal process driving high rates of submarine melting at tidewater glaciers. This buoyant discharge draws in warm seawater, entraining it in a turbulent upwelling flow along the submarine face that melts glacier ice. To capture the effects of subglacial discharge on submarine melting, we conducted 4 days of hydrographic transects during late summer 2012 at LeConte Glacier, Alaska. A major rainstorm allowed us to document the influence of large changes in subglacial discharge. We found strong submarine melt fluxes that increased from 9.1 ± 1.0 to 16.8 ± 1.3 m d^{-1} (ice face equivalent frontal ablation) as a result of the rainstorm. With projected continued global warming and increased glacial runoff, our results highlight the direct impact that increases in subglacial discharge will have on tidewater outlet systems. These effects must be considered when modeling glacier response to future warming and increased runoff. **Citation:** Motyka, R. J., W. P. Dryer, J. Amundson, M. Truffer, and M. Fahnestock (2013), Rapid submarine melting driven by subglacial discharge, LeConte Glacier, Alaska, *Geophys. Res. Lett.*, *40*, doi:10.1002/grl.51011.

1. Introduction

[2] Submarine melting impacts the stability of tidewater glaciers worldwide, but the connections between the ocean, a warming climate, and retreat of outlet glaciers are poorly known [*Straneo et al*., 2013]. Clearly warm seawater plays an important role, but the heat potential resident in oceans must be brought into contact with glacier termini in order to affect them. Accelerated mass loss from tidewater glaciers in Alaska, Greenland, and Antarctica is often attributed to dynamic changes initiated at the ice-ocean interface [*Rignot and Kanagaratnam*, 2006; *Howat et al*., 2007; *Nick et al*., 2009; *Post et al*., 2011]. For example, the current rates of glacier wastage in Alaska are some of the highest on the planet [*Radić and Hock*, 2011; *Gardner et al*., 2013], largely due to the rapid retreat of many tidewater glaciers [*Arendt et al*., 2006; *Larsen et al*., 2007]. Tidewater glaciers worldwide respond to ocean forcing in similar manners despite highly variable environmental settings [*Motyka et al*., 2003; *Thoma et al*., 2008; *Rignot et al*., 2010; *Motyka et al*., 2011; *Straneo et al*., 2011; *Sutherland and Straneo*, 2012; *Enderlin and Howat*, 2013]. Fjord circulation, driven by external ocean currents [*Straneo et al*., 2010], winds [*Straneo et al*., 2011], tides [*Mortensen et al*., 2011], and subglacial freshwater discharge [*Motyka et al*., 2003; *Rignot et al*., 2010; *Jenkins*, 2011; *Motyka et al*., 2011] can drive warm ocean water toward tidewater glaciers, melting them and, in some cases, triggering unstable retreat [*Holland et al*., 2008; *Motyka et al*., 2011]. Circulation within fjords and submarine melting are therefore important components of tidewater glacier mass balance, but they are arguably the least understood processes within these systems [*Straneo et al*., 2013]. This deficiency is due to the difficult environment that hinders comprehensive observations and the small spatial and temporal scales that are not yet resolvable in global circulation models.

[3] To help fill this knowledge gap, we conducted 4 days of hydrographic transects at LeConte Glacier, a grounded glacier in Southeast Alaska, during late summer 2012, a time when thermal forcing was high and subglacial discharge was vigorous. Because of the relatively simple geometry of the proglacial fjord, strong thermal forcings, large and variable subglacial discharge due to high surface melting and frequent heavy rainfall, and relative proximity to a logistical base, LeConte Glacier and Bay are exceptionally suitable for exploring glacier-fjord interactions. LeConte Glacier, 470 km^2 in area and 35 km long, funnels ice and subglacial water through a narrow 1 km-wide outlet and calves icebergs into 250 m deep water [*Motyka et al*., 2003]. The glacier is connected to Frederick Sound via LeConte Bay, a sill-dominated 24 km-long fjord (Figure 1a). Water exchange between the sound and bay occurs over a shallow barrier sill, S1, (10–15 m deep) at the entrance to the bay (Figure 1b). A second sill, S2, associated with the Little Ice Age advance, is 90 m deep and modulates water flow between the outer and inner fjord. The inner fjord reaches depths of 350 m and a third sill, S3, separates the deepest basin from the 250 m deep proglacial area. S3, 190 m at its deepest point, lies about 2 km from the present terminus and was the site of a 1962–1995 glacier standstill [*Motyka et al*., 2003].

2. Methods

[4] We performed three partial and eight complete hydrographic transects through a fluxgate over sill S3 (Figure 1c) during a 4 day period with acoustic Doppler current profilers (ADCP) and conductivity-temperature-depth (CTD) meters. Water fluxes were computed using heat and salt balance equations [*Motyka et al*., 2003; *Rignot et al*., 2010] (supporting

Additional supporting information may be found in the online version of this article.

[1]Geophysical Institute, University of Alaska Fairbanks, Fairbanks, Alaska, USA.
[2]Department of Natural Sciences, University of Alaska Southeast, Juneau, Alaska, USA.

Corresponding author: R. J. Motyka, Geophysical Institute, University of Alaska Fairbanks, 903 Koyukuk Drive, Fairbanks, AK 99775, USA. (rjmotyka@uas.alaska.edu)

0094-8276/13/10.1002/grl.51011

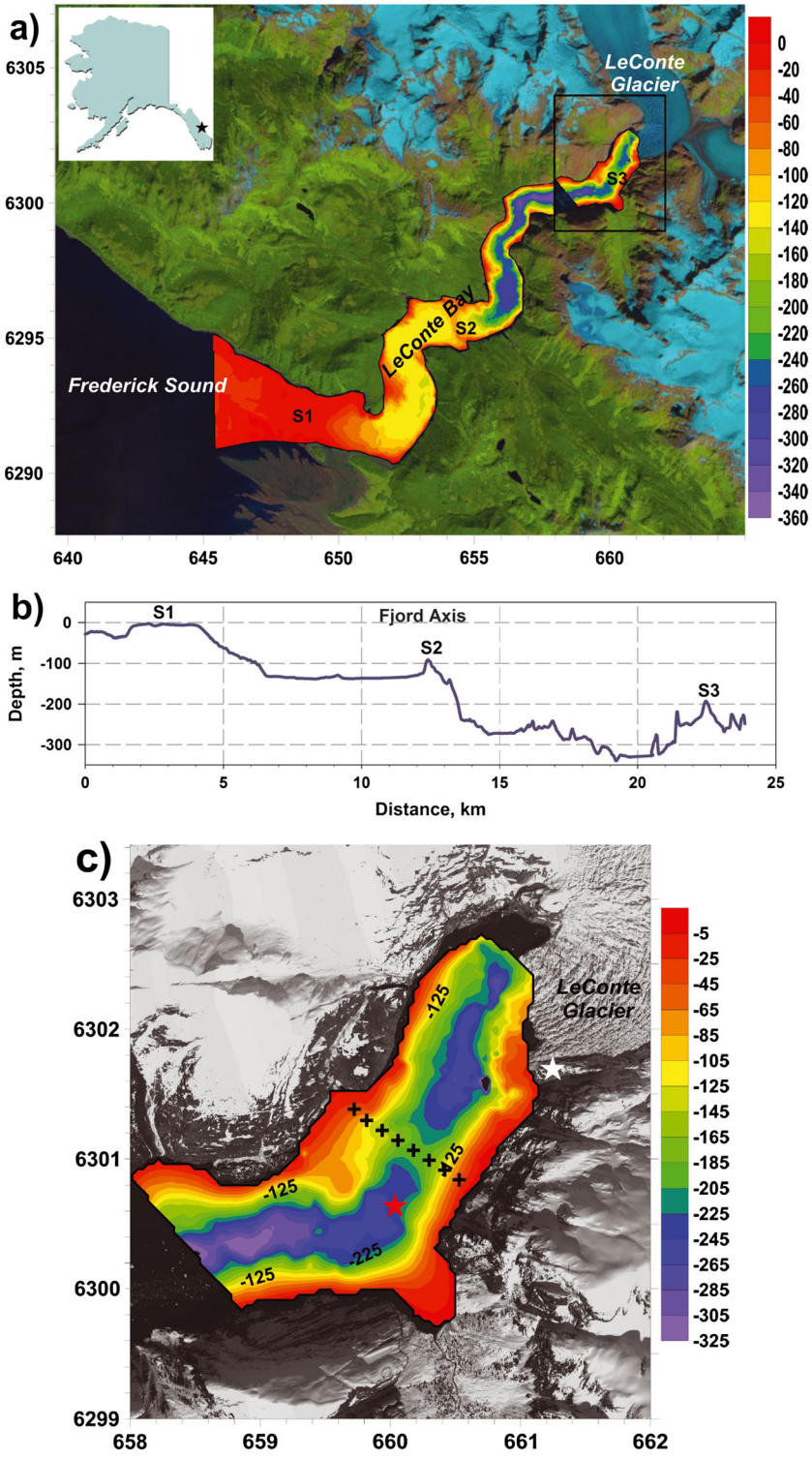

Figure 1. LeConte Glacier and Bay: (a) location and fjord bathymetry on Landsat 8 (10 August 2013), box indicates area depicted in Figure 1c; (b) depths and sills along fjord axis; (c) proglacial fjord with locations of fluxgate (crosses), mooring (red star), and camera (white star) on World View image (06 April 2012, Digital Globe, Inc.). Coordinates for Figures 1a and 1c are Universal Transverse Mercator km, zone 8.

information) based on the circulation model depicted in Figure 2. This method utilizes the fact that melting of glacier ice absorbs considerable thermal energy, the source of which is inferred to be incoming warm "ambient" seawater at depth. We used regularly spaced CTD casts and ADCP (600 kHz and 150 kHz) current measurements to parameterize water flowing through the 1.2 km wide gate. The fluxgate was close enough to the terminus to avoid complications of sidewall freshwater drainage into the fjord, yet far enough to avoid hazardous calving events, waves, and complications associated with plume turbulence at the face. Strong surface currents rapidly flushed icebergs down fjord, so we avoid complications associated

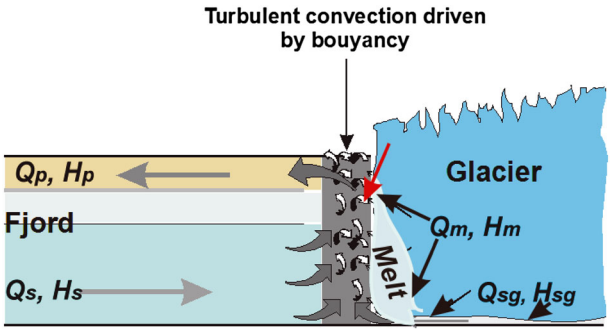

Figure 2. Model of proglacial convective flow at LeConte Glacier (modified from *Motyka et al*. [2003] with permission from International Glaciological Society). Subglacial discharge, Q_{sg}, carrying heat, H_{sg}, drives convection and draws deep saline water (Q_s, H_s) toward terminus where the two components mix and turbulently rise along the ice face. The ascending waters melt ice along the face (Q_m, H_m), which adds to convection. The turbulent plume reaches the water surface then flows away from the terminus in overflow plume (Q_p, H_p). Submarine undercutting of the terminus can lead to amplified calving of surface ice (red arrow).

with melting of icebergs. Each transect consisted of five to seven stations, spaced at an average of 190 m. Average time per station was 2.2 h (Table S2 in the supporting information). At each station, we lowered a SeaBird Electronics SeaCAT 19 "plus" CTD and used standard procedures to measure temperature, salinity, and turbidity of the water column that were depth-averaged into 1 m bins. We used a cantilevered, gunnel-mounted Teledyne RD 600 kHz ADCP to measure water currents in 2 m bins down to 70 m depth, missing the uppermost 4 m. We also used a 150 kHz RDI ADCP with bottom tracking as a back-up and to obtain currents at depth. The ADCPs were run consecutively for about 6min at each station. A "Hemisphere" GPS system provided real-time corrections for vessel drift and orientation. Comparison of the GPS navigation to ADCP bottom tracking positions showed excellent agreement.

[5] We simultaneously monitored the emergent outflow plume at the terminus using time-lapse photography at a 10-s frame rate. (Figure 1c and Videos S1–S4). A major rainstorm occurred on the second day of our transects (Figure S1) and significantly affected outflow.

[6] Our analyses of heat and salt balances and water fluxes are shown in the supporting information along with analysis of uncertainties. The analyses focus on the outflow plume and use 600 kHz ADCP measurements to evaluate fluxes (Figure 2). The fluxgate normal component was calculated and linearly interpolated vertically to 1 m and horizontally between stations to 10 m intervals. Currents for the top 4 m cannot be resolved by the ADCP and were therefore extrapolated from the bins immediately below. The depth of the outflow plume was determined from current, salinity, and temperature profiles and from analyses of submarine glacier meltwater content in the water column [*Mortensen et al*., 2013] (supporting information). The total water flux in the outflow plume, Q_p, was then calculated by integrating the measured, interpolated, and extrapolated currents across the fluxgate. End stations were usually within 150 m of bedrock shorelines; thus, some flow along the walls is missed by our stations.

3. Results and Discussion: Subglacial Discharge and Submarine Melting

[7] Table 1 provides results for eight fluxgate cross sections (three lacked sufficient data to characterize the entire cross section). Four of the eight transects were performed on day 2 to gauge tidal effects. Figure 3 shows four representative cross sections that highlight the daily changes in flux and water column characteristics (all remaining cross sections are in Figures S2–S5). The transects exhibit strong stratification in temperature, salinity, and water currents, as well as turbidity and meltwater content; these transitions help demarcate the outflow plume. Maximum temperatures (~6.9°C) typically occurred at depths of 85–95 m, compared to ~5°C in the plume. Mean temperature was slightly lower near the bottom of the fluxgate, ~6.8°C. Mean salinity, on the other hand, was greatest near the bottom of the water column (180 m), with values averaging ~28 versus 21–25 practical salinity unit in the plume. We used the mean temperature and salinity at ~180 m depth for "ambient seawater" in our calculations. Subglacial discharge (Q_{sg}), seawater entrainment (Q_{sw}), and submarine melting (Q_m), all increased significantly over the 4 days with Q_{sg} and Q_{sw} doubling (Table 1) and turbidity increasing tenfold (Figure 3 and supporting information). The corresponding submarine melt rates ranged from 9.1 ± 1.0 to -14.1 ± 1.2 m d^{-1} (ice face equivalent, mean values, averaged over the submarine face of the glacier) on days 1–3, then increased to 16.8 ± 1.3 m d^{-1} on day 4. Our results are the first in situ documentation of an increase in submarine melting with subglacial discharge. Given that subglacial discharge is

Table 1. Plume Fluxes (m^3/s)[a]

Transect Day, ID, Date[b], Start Time, ADT[c]	Q_p	Q_{sw}	Q_{fw}	Q_{sg}	Q_m	i. e. (m d^{-1})	Tide Stage	% uncertainty
1,T3, 9/7,14	2063	1917	146	130	15.6	−11.3	↑	10.7
2,T5, 9/8, 9	2022	1789	233	219	13.7	−9.1	—↓	11.4
2,T6, 9/8, 11	2856	2530	325	308	17.6	−11.9	↓—	9.3
2,T7, 9/8, 12.5	2376	2099	277	263	14.1	−9.5	—↑	9.8
2,T8, 9/8, 14.5	2949	2676	273	254	19.5	−14.1	↑	8.5
3,T9, 9/9, 9	2497	2301	197	177	19.4	−13.2	—↓	11.0
3,T10, 9/9, 11.5	2815	2554	261	243	17.9	−12.5	↓—	9.5
4,T11, 9/10, 13	4528	4065	463	439	24.9	−16.8	—↓	8.0

[a] Q_p = total flux in plume, Q_{sw} = seawater, Q_{fw} = freshwater, Q_{sg} = subglacial discharge, Q_m = submarine melting. Also listed are the ice equivalent (i. e.) frontal ablation of glacier submarine face in m d^{-1}, tide stage during survey (↑ = rising, ↓ = ebbing, — = slack), and relative uncertainties (discussed in the supporting information).
[b] Dates are formatted as month/day.
[c] ADT = Alaska Daylight Time.

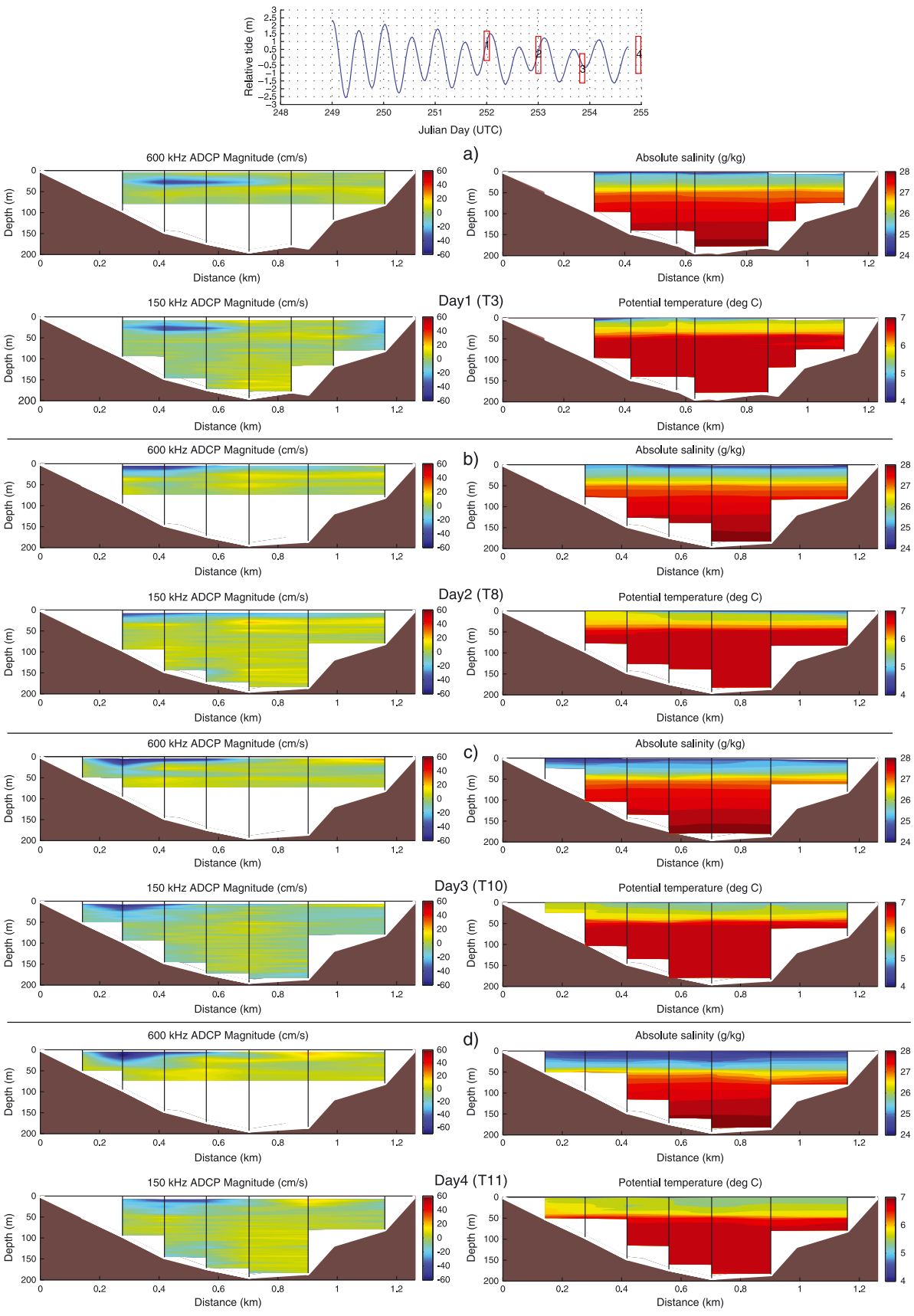

Figure 3. Representative cross sections for each day of surveys. (left column) The 600 and 150 kHz ADCP data, and (right column) salinity and temperature. (a) Day 1 (T3), (b) Day 2 (T8), (c) Day 3 (T10), and (d) Day 4 (T11). Additional data in Table 1. Complete set of cross sections can be found in the supporting information. Tides are from our nearby mooring (Figure 1c); numbers and red bars correspond to the transects by day number.

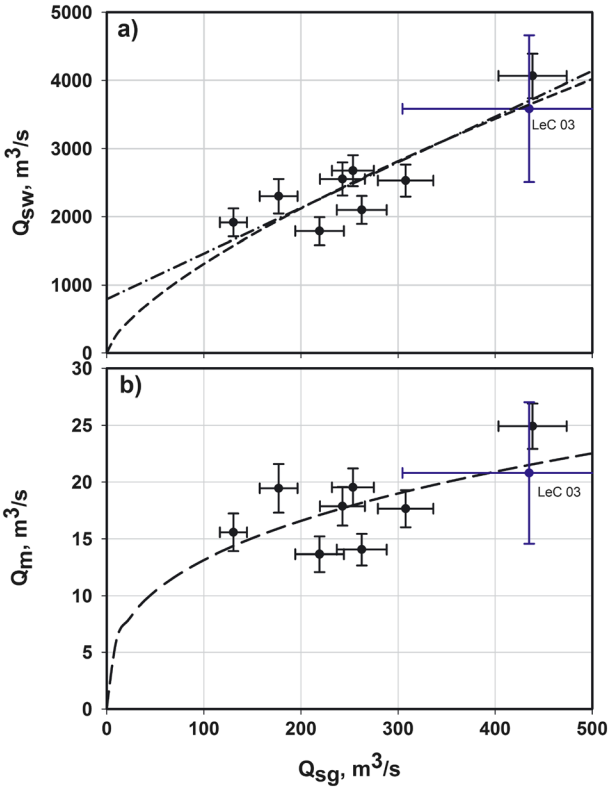

Figure 4. LeConte Glacier: (a) Seawater flux (Q_{sw}) as a function of subglacial discharge (Q_{sg}). Dash-dotted line is linear fit; dashed line is two-thirds power fit to data; (b) subglacial melting (Q_m) as a function of subglacial discharge. Dashed line is one-third power fit to data. Results from *Motyka et al.* [2003] also included (blue).

likely to increase in a warming climate, the relationship between discharge and melting observed at LeConte Glacier has important implications for marine-terminating glaciers.

[8] We ascribe the large increases in subglacial discharge and turbidity to the rainstorm, and the dramatic changes on day 4 to an outburst of subglacially stored water following this storm, which flushed subglacial sediment. Our time-lapse videos (Videos S1–S4) also capture these large fluctuations in outflow and turbidity. Waves of turbulent emergent flow can be readily seen during all days but were strongest during day 4 of observations. Plumes occurred along the entire face but were strongest along the northwest half. The outflow continued through our fluxgate and produced a broad surface eddy beyond the gate that was captured in our surveys.

[9] We attribute shorter term fluctuations (days 2 and 3, Table 1) to tidally driven hydrostatic pressure changes, variations in precipitation, and diurnal glacier surface ablation. Our surveys bracketed the neap tide with amplitudes on day 2 of ~1.4 m for ebb and ~2.0 m for flood; day 3 ebb amplitude was ~1.1 m. In comparison, spring tide amplitudes are 3 to 4 times these values. On day 2, all fluxes increased during the ebb tide (T5–T6), then began dropping at the start of the flood tide (T7), but later increased significantly (T8). On the following day during the ebb, fluxes followed a similar pattern except that submarine melting remained constant within uncertainty limits. We attribute the increases in flux during the ebbing tide to a drop in hydrostatic pressure at the glacier terminus, allowing increased release of subglacial discharge. Later in the day, we suspect that subglacial discharge from increased precipitation eventually overwhelmed the tidal signal, causing fluxes to increase despite a rising tide. Alternately, the increased flux could be due to release of stored water and/or diurnal variations in surface ablation.

[10] Figure 4 illustrates that subglacial discharge is the engine that drives influx of warm seawater to melt submarine glacier ice in LeConte Bay. Figure 4a shows a strong linear trend ($R^2 = 0.76$) between subglacial discharge and seawater influx, but the trend does not pass through the origin, suggesting the action of some additional currents, perhaps tidal, wind, or thermohaline. Curve fitting with a two-thirds power relationship forces the fit through the origin and also shows good correlation ($R^2 = 0.78$). *Jenkins* [2011] suggested a one-third power relationship between submarine melting and subglacial discharge (dashed line in Figure 4b, $R^2 = 0.37$). We suspect the scatter in the data reflects complexities in the turbulent upwelling at the submarine face [*Jenkins*, 2011; *Xu et al.*, 2012]. In addition to confirming our 2003 findings [*Motyka et al.*, 2003], the submarine melt rates from this study are comparable to a similar 1983 study at Alaska's Columbia Glacier, where thermal forcing was ~11.5°C and Q_m ranged from 18 to 50 $m^3\,s^{-1}$ [*Walters et al.*, 1988]. Our ice equivalent frontal ablation rates due to submarine melting are 2 to 3 times those found for Greenland glaciers [*Rignot et al.*, 2010; *Motyka et al.*, 2011; *Sutherland and Straneo*, 2012; *Enderlin and Howat*, 2013], where thermal forcing is substantially lower (~ 1–4°C) and termini are wider. Together, these studies highlight the importance of submarine melting at marine-terminating glaciers. At LeConte Glacier, the total frontal ablation rate (calving flux plus submarine melting) is ~3.0×10^6 $m^3\,d^{-1}$ (water equivalent), which far surpasses surface ablation [*Motyka et al.*, 2003; *O'Neel et al.*, 2003]. Ice speeds at the terminus range from 20 to 25 $m\,d^{-1}$, compared to our melting rates of 9.1 to 16.8 $m\,d^{-1}$. Our results therefore indicate that about one half to two thirds of the frontal ablation during September 2012 can be attributed to submarine melting.

4. Conclusions

[11] Our measurements revealed that subglacial discharge rose from 130 to 440 $m^3\,s^{-1}$ between 07 and 10 September 2012 as a result of a major rainstorm. These increases in Q_{sg} escalated convective influx of warm seawater (thermal forcing ~8°C): from 1800 to 4000 $m^3\,s^{-1}$. As a result, submarine melt fluxes almost doubled over the 4 day period: from 14 to 25 $m^3\,s^{-1}$ (9.1 ± 1.0 to 16.8 ± 1.3 $m\,d^{-1}$ ice equivalent terminus melt).

[12] Our results support a previously invoked two-layer model driven by buoyant subglacial freshwater [*Motyka et al.*, 2003; *Rignot et al.*, 2010], but we also see evidence of eddying both at the terminus and down fjord, adding complexity to this simple model. Our results establish turbulent subglacial discharge as a key driver of ice-proximal fjord circulation that entrains warm seawater and melts submarine glacial ice. Submarine undercutting of the terminus may also lead to increased calving of surface ice [*O'Leary and Christoffersen*, 2013]. Our results show that tidewater glacier dynamics and hence ice sheet stability are not only directly affected by increased surface ablation and higher ocean temperatures but also through increased proglacial fjord circulation driven by increases in glacial runoff; a result that is also

evident in models [*Jenkins*, 2011; *Xu et al*., 2012]. This has direct implications for predicting future behavior at the ice sheet ocean interface, which constitutes the major uncertainty for predictions of ice loss and sea level rise [*Straneo et al*., 2013; *Bindschadler et al*., 2013].

[13] **Acknowledgments.** This work was funded by a grant from the Gordon and Betty Moore Foundation grant GBMF2627 to M.T. and M.F. Additional support for J.M.A. was provided by NSF grant ANT0944193. The manuscript was greatly improved by comments from two anonymous reviewers. We thank Captain Scott Hursey for vessel support and safely navigating us through icebergs. J. Elliot provided the orthorectified World View image in Figure 1c.

[14] The Editor thanks Ellyn Enderlin and an anonymous reviewer for their assistance in evaluating this paper.

References

Arendt, A., K. Echelmeyer, W. Harrison, C. Lingle, S. Zirnheld, V. Valentine, B. Ritchie, and M. Druckenmiller (2006), Updated estimates of glacier volume changes in the western Chugach Mountains, Alaska, and a comparison of regional extrapolation methods, *J. Geophys. Res.*, *111*, F03019, doi:10.1029/2005JF000436.

Bindschadler, R. A., et al. (2013), Ice-sheet model sensitivities to environmental forcing and their use in projecting future sea level (the SeaRISE project), *J. Glaciol.*, *59*(214), 195–224, doi:10.3189/2013JoG12J125.

Enderlin, E. M., and I. M. Howat (2013), Submarine melt rate estimates for floating termini of Greenland outlet glaciers (2000–2010), *J. Glaciol.*, *59* (*213*), 67–75, doi:10.3189/2013JoG12J049.

Gardner, A. S., et al. (2013), A reconciled estimate of glacier contributions to sea level rise: 2003 to 2009, *Science*, *340*(6134), 852–857, doi:10.1126/science.1234532.

Holland, D., R. H. Thomas, B. de Young, and M. H. Ribergaard (2008), Acceleration of Jakobshavn Isbrae triggered by warm subsurface ocean waters, *Nat. Geosci.*, *1*, 659–664.

Howat, I., I. Joughin, and T. A. Scambos (2007), Rapid changes in ice discharge from Greenland outlet glaciers, *Science*, *315*, 1559–1561.

Jenkins, A. (2011), Convection-driven melting near the grounding lines of ice shelves and tidewater glaciers, *J. Phys. Oceanogr.*, *41*, 2279–2294.

Larsen, C. F., R. J. Motyka, A. A. Arendt, K. A. Echelmeyer, and P. E. Geissler (2007), Glacier changes in southeast Alaska and northwest British Columbia and contribution to sea level rise, *J. Geophys. Res.*, *112*, F01007, doi:10.1029/2006JF000586.

Mortensen, J., K. Lennert, J. Bendtsen, and S. Rysgaard (2011), Heat sources for glacial melt in a sub-Arctic fjord (Godthåbsfjord) in contact with the Greenland Ice Sheet, *J. Geophys. Res.*, *116*, C01013, doi:10.1029/2010JC006528.

Mortensen, J., J. Bendtsen, R. J. Motyka, K. Lennert, M. Truffer, M. Fahnestock, and S. Rysgaard (2013), On the seasonal freshwater stratification in the proximity of fast-flowing tidewater outlet glaciers in a sub-Arctic sill fjord, *J. Geophys. Res. Oceans*, *118*, 1382–1395, doi:10.1002/jgrc.20134.

Motyka, R., L. Hunter, K. Echelmeyer, and C. Connor (2003), Submarine melting at the terminus of a temperate tidewater glacier, LeConte Glacier, Alaska, USA, *Ann. Glaciol.*, *36*, 57–65.

Motyka, R. J., M. Truffer, M. Fahnestock, J. Mortenson, S. Rysgaard, and I. Howat (2011), Submarine melting of the 1985 Jakobshavn Isbrae floating ice tongue and the triggering of the current retreat, *J. Geophys. Res.*, *116*, F01007, doi:10.1029/2009JF001632.

Nick, F. M., A. Vieli, I. M. Howat, and I. Joughin (2009), Large-scale changes in Greenland outlet glacier dynamics triggered at the terminus, *Nat. Geosci.*, *2*, 110–114.

O'Leary, M., and P. Christoffersen (2013), Calving on tidewater glaciers amplified by submarine frontal melting, *Cryosphere*, *7*, 119–128, doi:10.5194/tc-7-119-2013.

O'Neel, S., K. Echelmeyer, and R. J. Motyka (2003), Short-term variations in calving at a retreating tidewater glacier: LeConte Glacier, Alaska, *J. Glaciol.*, *49*(167), 587–598.

Post, A., S. O'Neel, R. J. Motyka, and G. Streveler (2011), A complex relationship between calving glaciers and climate, *EOS Trans. AGU*, *82*(37), 305–312.

Radić, V., and R. Hock (2011), Regionally differentiated contribution of mountain glaciers and ice caps to future sea-level rise, *Nat. Geosci.*, *4*(2), 91–94, doi:10.1038/ngeo1052.

Rignot, E., and P. Kanagaratnam (2006), Changes in the velocity structure of the Greenland Ice Sheet, *Science*, *311*, 986–990.

Rignot, E., M. Koppes, and I. Velicogna (2010), Rapid submarine melting of the calving faces of West Greenland glaciers, *Nat. Geosci.*, *3*, 187–191.

Straneo, F., G. S. Hamilton, D. A. Sutherland, L. A. Stearns, F. Davidson, M. O. Hammill, G. B. Stenson, and A. Rosing-Asvid (2010), Rapid circulation of warm subtropical waters in a major, East Greenland glacial fjord, *Nat. Geosci.*, *3*, 182–186.

Straneo, F., R. Curry, D. A. Sutherland, G. Hamilton, C. Cenedese, K. Väge, and L. A. Stearns (2011), Impact of fjord dynamics and subglacial discharge on the circulation near Helheim Glacier, *Nat. Geosci.*, *4*, 332–327, doi:10.1038/ngeo1109.

Straneo, F., et al. (2013), Challenges to understand the dynamic response of Greenland's marine terminating glaciers to oceanic and atmospheric forcing, *Bull. Am. Meteorol. Soc.*, *94*, 1131–1144, doi:10.1175/BAMS-D-12-00100.

Sutherland, D., and F. Straneo (2012), Estimating ocean heat transports and submarine melt rates in Sermilik Fjord, Greenland, using lowered ADCP velocity profiles, *Ann. Glaciol.*, *53*(60), 50–58.

Thoma, M., A. Jenkins, D. Holland, and S. Jacobs (2008), Modelling circumpolar deep water intrusions on the Amundsen Sea continental shelf, Antarctica, *Geophys. Res. Lett.*, *35*, L18602, doi:10.1029/2008GL034939.

Walters, R. A., E. G. Josberger, and C. L. Driedger (1988), Columbia Bay, Alaska: An "upside down" estuary, *Estuarine Coastal Shelf Sci.*, *26*(6), 607–617.

Xu, Y., E. Rignot, D. Menemenlis, and M. Koppes (2012), Numerical experiments on subaqueous melting of Greenland tidewater glaciers in response to ocean warming and enhanced subglacial discharge, *Ann. Glaciol.*, *53*(60), 229–234.